AGU ADVANCING EARTH AND SPACE SCIENCE

Geophysical Research Letters

RESEARCH LETTER
10.1029/2021GL094485

Reconciling Debates on the Controls on Surface Urban Heat Island Intensity: Effects of Scale and Sampling

Jiameng Lai[1], Wenfeng Zhan[1,2], Jinling Quan[3], Zihan Liu[1], Long Li[1], Fan Huang[1], Falu Hong[1], and Weilin Liao[4]

[1]Jiangsu Provincial Key Laboratory of Geographic Information Science and Technology, International Institute for Earth System Science, Nanjing University, Nanjing, Jiangsu, China, [2]Jiangsu Center for Collaborative Innovation in Geographical Information Resource Development and Application, Nanjing, China, [3]State Key Laboratory of Resources and Environmental Information System, Institute of Geographic Sciences and Natural Resources Research, Chinese Academy of Sciences, Beijing, China, [4]Guangdong Key Laboratory for Urbanization and Geo-simulation, School of Geography and Planning, Sun Yat-sen University, Guangzhou, China

Key Points:

- Contributions from climate condition to surface urban heat island intensity (SUHII) gradually decrease with increasing temporal scale
- No common rank exists in the relative importance of main types of SUHII controls over different spatial scales
- Sampling style of city cluster by urban area or climate zone contributes to debates on ranks of SUHII controls

Supporting Information:

Supporting Information may be found in the online version of this article.

Correspondence to:

W. Zhan,
zhanwenfeng@nju.edu.cn

Citation:

Lai, J., Zhan, W., Quan, J., Liu, Z., Li, L., Huang, F., et al. (2021). Reconciling debates on the controls on surface urban heat island intensity: Effects of scale and sampling. *Geophysical Research Letters*, *48*, e2021GL094485. https://doi.org/10.1029/2021GL094485

Received 1 JUN 2021
Accepted 13 SEP 2021

Abstract

Variations in the surface urban heat island intensity (SUHII) are regulated mainly by three types of control: surface property, background climate (or weather) conditions, and overall urban metric. However, intensive debates arise over the relative importance of these three control types. Here, over 896 Chinese city clusters, we reconcile these debates by showing that the priorities of the three SUHII control types depend closely on the scale and sampling criteria, although they are all crucial in regulating SUHII variations. With increasing temporal scale, the contributions from climate (or weather) conditions decrease, while those from surface property and overall urban metric increase. We find no consistent ranking in the relative importance of these three control types on various spatial scales. The sampling style of city cluster also contributes to disagreements regarding SUHII controls. Our findings potentially help resolve the long-standing debate on the relative importance of SUHII controls.

Plain Language Summary

Surface urban heat islands (SUHIs) have a profound impact on the lives of urban residents. Previous studies have suggested three major types of factors that control SUHI intensity (SUHII) variations: surface property, background climate (or weather) conditions, and overall urban metric. Debates however appear over the priorities of these three types of factors on regulating SUHIIs, and the lack of studies that can reconcile these debates has hindered significantly the in-depth understanding of the SUHII mechanisms. Through an empirical analysis of the SUHII controls, our results show that these three types of factors are all indispensable in regulating the SUHII variations; and their priorities closely depend on the scale and sampling style. Furthermore, this study summarizes the types of factors that matter the most to the SUHIIs under different scenarios, and therefore has the potential to help develop the most efficient SUHI mitigation strategies.

1. Introduction

More than half of the world's population now lives in cities and most of this population is exposed to the urban heat island (UHI) effect (Grimmond, 2007). The UHI effect is exerted on the subsurface, surface, canopy, and boundary layers (F. Huang et al., 2020; Oke et al., 2017). The accumulation of satellite data has resulted in an upsurge in surface UHI (SUHI) investigations in recent decades (D. Zhou et al., 2019).

The interpretation of the SUHI requires an in-depth understanding of its controls and their relative importance (J. Peng et al., 2018; D. Zhou et al., 2019). The SUHI has been long attributed to the urban-rural difference in surface property, i.e., the local properties of the land surface at pixel/landscape scale, such as land cover type, surface structure, and landscape configuration (Chen et al., 2006; Lazzarini et al., 2015; Weng, 2009; Yuan & Bauer, 2007). During the day, more solar radiation is converted to sensible heat over urban impervious surfaces, resulting in the SUHI (Yow, 2007). Typical building structures such as urban canyons contribute to the nighttime SUHI by suppressing nocturnal cooling (Lai et al., 2018; Scarano & Sobrino, 2015). Variations of SUHI intensity (SUHII) also depend on the configuration of buildings and vegetation (W. Zhou, Huang, et al., 2011). Using satellite observations, the urban-rural contrast in surface property has been shown to control both inner- and inter-city SUHII variations and their monthly and yearly dynamics (Scarano & Sobrino, 2015; Schwarz & Manceur, 2015; Yao, Wang, Gui, et al., 2017; Yao et al., 2019).

The traditional concept that the SUHII is regulated mainly by the urban-rural contrast in surface property has been challenged by two categories of study. One category argues that SUHII variations are regulated more by background climate (e.g., temperature and precipitation which represent the atmospheric condition of the region in which the city is located; Zhao et al., 2014). The background climate (or weather) can have a decisive effect on SUHII variations across different climate zones, and on the SUHII day-to-day dynamics, mainly via regulating convective, radiative, and evaporative processes (Cao et al., 2016; Hu, 2021; Lai et al., 2021; Zhao et al., 2014; J. Zhou, Chen, et al., 2011). The other category of study attributes SUHII variations to overall urban metric, i.e., the metrics that can describe the urban level/scale of the entire city, e.g., urban size, population, and energy consumption (X. Li et al., 2017; Liao et al., 2017). Cities with a higher urban level (e.g., with a larger size or denser population) tend to experience a more intense SUHII (X. Li et al., 2017; Liao et al., 2017; Manoli et al., 2019; B. Zhou et al., 2013).

An intense debate has been fueled by various studies that suggest different rankings of the importance of these three SUHII control types – surface property, background climate, and overall urban metric (e.g., Manoli et al., 2019; S. Peng et al., 2012; Weng et al., 2004; Zhao et al., 2014; Figure S1 and Table S1). Even for the same control, its impact on the SUHII varies. While city size has been reported to be important in regulating SUHII variations (Clinton & Gong, 2013; Imhoff et al., 2010; X. Li et al., 2017; B. Zhou et al., 2013), several studies have suggested the opposite (Heinl et al., 2015; S. Peng et al., 2012; D. Zhou et al., 2014). Some studies have reported that precipitation has a negative effect on SUHII (Lai et al., 2021; J. Zhou, Chen, et al., 2011), while others have indicated an intensifying effect (Zhao et al., 2014). The lack of studies providing an explanation for these conflicting findings hinders an in-depth understanding of SUHII mechanisms, and it impedes the communication of the true importance of various SUHII controls within the urban climate community.

Here, we attempt to reconcile these different conclusions and to resolve the debate. We investigated 896 city clusters in China, within a wide range of climate zones (Figure S2), in order to determine the relative importance of the three types of SUHII control for different scales and sampling criteria. We show that the contradictory findings can largely be explained by scale effects in space and time, together with the sampling criteria for city clusters. Finally, we consider the implications of our findings for SUHII mechanisms and on communication within the literature.

2. Materials and Methods

2.1. Materials

The city cluster boundary data were obtained from Natural Earth (1:10 m vectors, v4.1.0, http://www.naturalearthdata.com), and were generated by combining the global urban extent map and the LandScan population database. We chose city clusters in China as the study area due to its vast territory, wide variety of climate zones (Zheng et al., 2010), and rapid urbanization in the past few decades (Luo & Lau, 2018; Yang et al., 2017; L. Zhou et al., 2004). A total of 1,327 city clusters were first identified with the urban boundary data set; whereas only 896 clusters with urban areas >10 km^2 during 2003–2018 were selected (see Quantification of the SUHI). The distributions of the city clusters are shown in Figure S2. The population data (2003–2018) were from LandScan™ (https://landscan.ornl.gov) and possess a spatial resolution of 1 km. Such data were generated by combining land cover type, nighttime light, and high-resolution panchromatic imagery (Dobson et al., 2000).

The MODIS data set (version 6, 2003–2018) was employed in this study. It includes land cover type, land surface temperature (LST), enhanced vegetation index (EVI), and albedo products (Table S2). The land cover type product (MCD12Q1) has a spatial resolution of 500 m. LST was derived from the daily product MOD11A1 onboard the Terra satellite (acquired at 10:30 and 22:30 local time) and MYD11A1 onboard the Aqua satellite (acquired at 13:30 and 01:30 local time). The LST data have a spatial resolution of 1 km, and their retrieval errors are <1.0 K under most conditions (Wan, 2008). To reduce the impact of missing data contaminated by clouds, we composited the daily LSTs obtained at 10:30 and 13:30 as daytime LSTs, and composited those obtained at 22:30 and 01:30 as nighttime LSTs (Du et al., 2016; B. Zhou et al., 2017). The

EVI data were from the 16 day product MOD13A2, with a spatial resolution of 1 km. The albedo data were derived from the MCD43A3 product with a spatial resolution of 500 m.

We used the global atmospheric reanalysis data ERA-Interim (https://www.ecmwf.int/en/forecasts/datasets/reanalysis-datasets/era-interim) to obtain the meteorological variables (Dee et al., 2011). The ERA-Interim data have a spatial resolution of 0.125°. The associated variables include total column water vapor, horizontal wind speed (at 10 m), accumulated precipitation, and surface air temperature. Daily values at local time 8:00 (as daytime values) and 20:00 (as nighttime values) from 2003 to 2018 were used.

2.2. Quantification of SUHI

We quantified the SUHI using the indicator SUHII, defined as the mean LST difference between urban and rural areas (Voogt & Oke, 2003). Delineation of urban and rural areas is needed before the calculation of the SUHII. The extent of each city cluster was first enlarged using a buffer zone with a distance equal to the radius of the original city cluster polygon, as the original city cluster was identified based on the 2002 MODIS land cover map while rapid and extensive urbanization has taken place in China after 2002. Within each derived cluster, the pixels classified as "built-up" by the land cover product (i.e., MCD12Q1) were then regarded as urban areas; whereas the other pixels were regarded as rural (Chakraborty & Lee, 2019). In this study, pixels classified as water bodies were excluded from the analysis (Chakraborty & Lee, 2019).

2.3. Selection of SUHII Controls

The selection of SUHII controls was based on two criteria: (a) the factor should demonstrate significant temporal dynamics (to explain the SUHII dynamics) and/or spatial variations (to explain city-by-city SUHII variations); and (b) the factor is easily quantifiable with satellite or reanalysis data. A total of eight variables were selected as SUHII controls (see Table S3). They include the urban-rural contrast in EVI and albedo (termed ΔEVI and ΔALB respectively), which are components of the surface property; total column water vapor (termed TWV); horizontal wind speed at 10 m (termed WDS); surface air temperature (termed SAT) and accumulated precipitation (termed PREP), which are components of the background climate (or weather) conditions; and urban area (termed UA) and population (termed POP), which are components of overall urban metric (Lai et al., 2021; S. Peng et al., 2012; B. Zhou et al., 2013). For each city cluster, ΔEVI and ΔALB were calculated as the mean difference in EVI or albedo between urban and rural areas; TWV, WDS, SAT, PREP, and POP were calculated as their mean values within the extent of each city cluster; and UA was calculated as the area of urban pixels in each city cluster. Daily values of each variable were derived. For ΔEVI and ΔALB with a temporal resolution coarser than 1 day, the daily values were calculated as their nearest observations. For UA and POP, the daily values across each year were estimated as their yearly values.

2.4. Determining the Relative Importance of SUHII Controls

We chose the regression tree (RT) model to quantify the relationships between SUHII and associated controls, as well as the relative importance of each category of control (Wang et al., 2015). All the controls in Table S3 were used as input variables to the RT model to fit the SUHII, and the contribution of each control was estimated as the average change in the fitted mean squared error due to each split in that control in the RT model (see Text S1 for more details). To facilitate comparison, the contributions were normalized to 0 to 1.0 by dividing by the sum of the contribution from all controls. The relative importance of each group of controls (Logan et al., 2020; W. Zhou, Huang, et al., 2011) was finally estimated as the sum of the normalized contribution of all the controls belonging to the associated group.

We designed three scenarios to investigate the relative importance of each type of control for various spatiotemporal scales and sampling criteria (Table S4). To avoid statistical unreliability induced by a small sample size, at least 30 pairs of SUHII and associated controls are needed for RT modeling (Maccallum et al., 1999), except for the analysis over the yearly scale as only 16 yr of data are available for regression. Those with insufficient samples were removed from further analysis.

In Scenario #1, controls of SUHII dynamics were analyzed at different temporal scales, including day-to-day, daily, monthly, and yearly scales (see Figure S3). We estimated the relative importance of each SUHII control for each city cluster at each scale (Lai et al., 2021; Yao, Wang, Huang, et al., 2017). For the monthly and yearly scales, the monthly and yearly means of each variable were used as input for the RT model. For the day-to-day scale, the values of variables were calculated as the differences between their daily values and the corresponding monthly means. To avoid cloud impacts, the daily and day-to-day values on days with >60% of urban or rural LSTs contaminated by clouds were removed from the analysis (Figure S4).

In Scenario #2, the controls on spatial variations in SUHII were analyzed over different spatial scales. Here, the city-by-city SUHII variations within moving grids with different sizes are referred to as the spatial SUHII variations on different spatial scales. The investigated spatial scales are: 5° × 5° (grid size), 10° × 10°, and 15° × 15°, together with the scale that incorporates all the city clusters within the entire landmass of China (Figure S5). The central latitude and longitude for each moving grid are given in Table S5. Most grids are in central or eastern China because the number of city clusters in western China is more likely to be too low to satisfy the requirement for fitting the RT model. At each spatial scale, the RT model was fitted based on the SUHII and controls over the city clusters within each corresponding grid. In this scenario, for each city cluster, the SUHII and associated controls were calculated by averaging all the daily values across the study period.

In Scenario #3, controls on spatial SUHII variations were analyzed with different sampling criteria. City clusters were sampled from both the temporal and spatial perspectives, and the SUHIIs for the sampled city clusters were fitted using the RT model. From the temporal perspective, city clusters were sampled by "summer days", "winter days", and "all-year days" (S. Peng et al., 2012; Shastri et al., 2017); while from the spatial perspective, sampling was conducted either by urban area (X. Li et al., 2017) or by background climate (Ward et al., 2016; D. Zhou et al., 2014). For sampling by urban area, the 896 city clusters were classified into 10 groups (termed "UA01" to "UA10"), each with almost the same number of cities but with an increasingly urban area. For sampling by background climate, only 856 city clusters in five climate zones (i.e., south subtropical, mid subtropical, north subtropical, warm temperate, and mid temperate, from south to north) were involved, while the remaining 40 city clusters were disregarded as the cluster numbers in the other climate zones were too small to be included in the RT model.

3. Results and Discussion

3.1. Impact of Temporal Scale on SUHII Controls

Assessment of the relative importance of various SUHII controls demonstrates that weather conditions dominate SUHII dynamics on shorter timescales (e.g., day-to-day and daily scales, Figure 1). Among the meteorological variables, water vapor and air temperature have the closest relationship with SUHII dynamics (Figure S6). The strong dependence of the day-to-day SUHII dynamics on weather condition, especially on water vapor which can generally suppress the SUHII mainly by reducing the radiation load of the land surface, is consistent with previous conclusions (Lai et al., 2021; W. Zhou, Huang, et al., 2011). On longer timescales (e.g., monthly and especially yearly), by comparison, the surface property and overall urban metric also regulate the SUHII dynamics, although climate condition remains a major contributor (Figure 1).

Specifically, on the day-to-day scale, the relative importance of the three types of control shows small between-city deviations and small daytime-nighttime contrasts (Figure 1). For all the cities, weather conditions make the largest contribution (about 55%–75%) to SUHII dynamics, yet the contributions from the surface property (20%–35%) and overall urban metric (less than 10%) are much lower (Figures 1a and 1b). On the daily and monthly scales, the contributions from climate (or weather) conditions remain principal on nighttime SUHII dynamics (Figures 1d and 1f). However, daytime SUHII dynamics are more regulated by surface property in a small portion of the cities, especially those within the WT, AT, and MT climate zones (Figures 1c and 1e). This result corresponds to the previously reported large impacts from seasonal land cover changes induced by vegetation phenology on the daytime SUHII (Haashemi et al., 2016; Lazzarini et al., 2013). On the yearly scale, there is no common ranking of the contributions from the three types of control–each can be the most important (Figures 1g and 1h) and their ranks deviate among different city clusters (Figure S7).

10.1029/2021GL094485

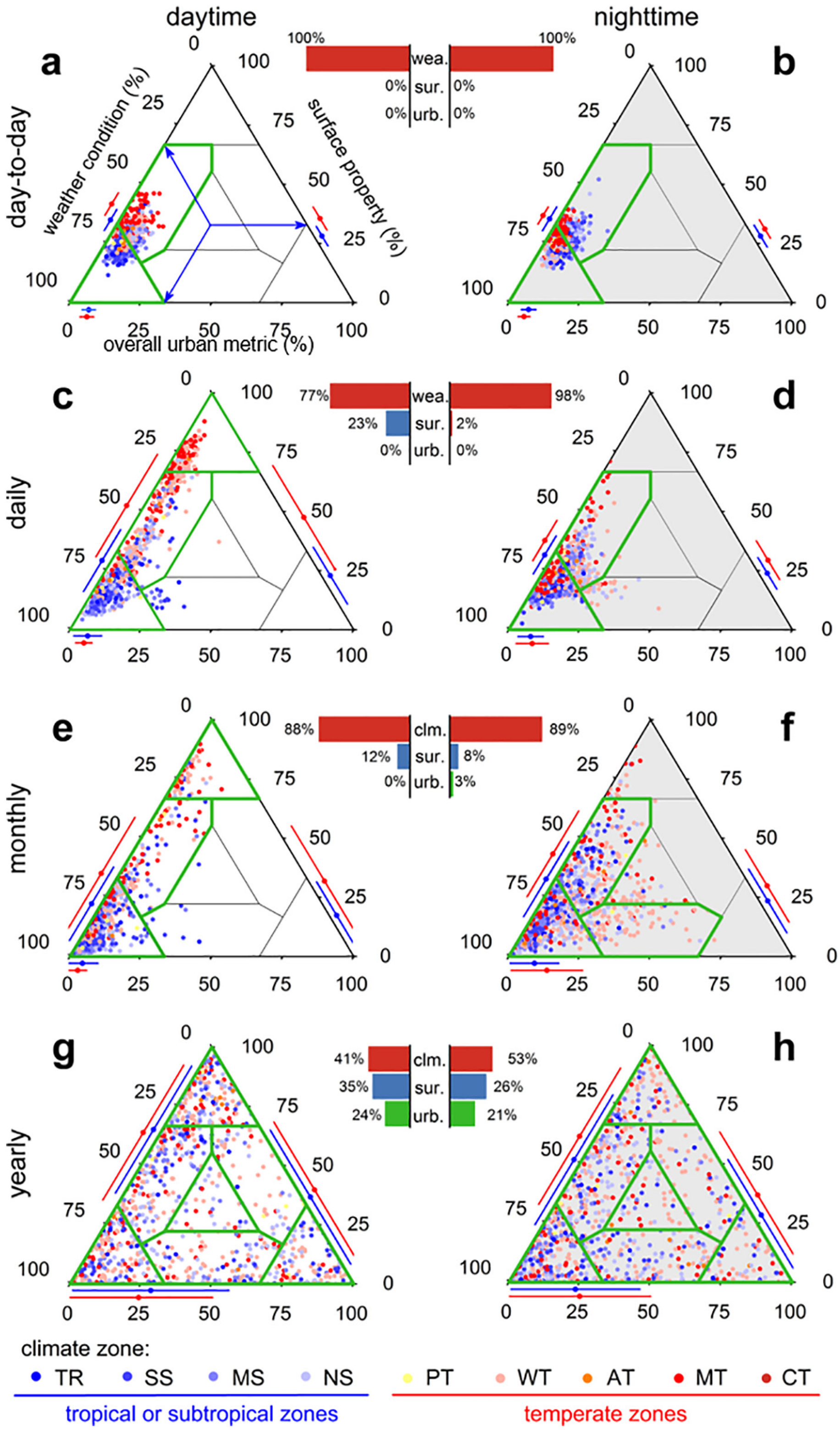

Figure 1.

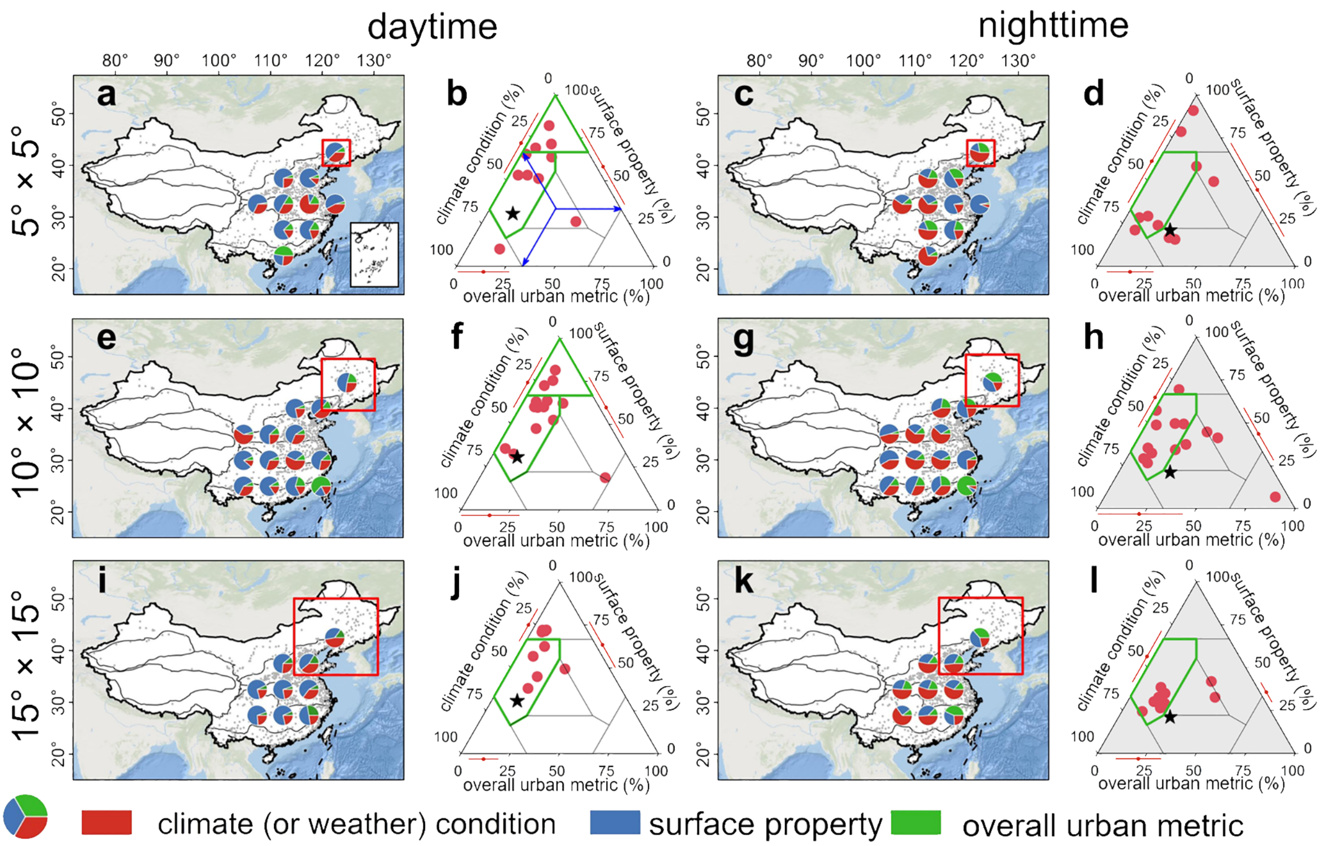

Figure 2. Relative importance of the three types of SUHII control on different spatial scales, indicated by moving grid size. The three moving grid sizes are: 5° × 5°, 10° × 10°, and 15° × 15°. The first and third columns display the contributions of the three SUHII control types for each moving grid during the day and at night, respectively, with the red boxes illustrating the moving grid size and the central longitude/latitude of each grid given in Table S5. The second and fourth columns are the triangle diagrams for the relative importance of these SUHII control types over all the moving grids at the corresponding scale during the day and at night, respectively. The black stars in the triangle diagrams denote the relative importance of SUHII controls for the whole of China.

The contribution analysis in Figures 1 and S6 provides empirical evidence for the notable dependence of the SUHII controls on the temporal scales. This result helps resolve the debate regarding the dominant SUHII controls suggested in previous studies, which focused on different temporal scales (Table S1), including day-to-day and daily (Lai et al., 2021; Shaposhnikova, 2018; W. Zhou, Huang, et al., 2011), monthly and seasonal (Haashemi et al., 2016; Lazzarini et al., 2013), and yearly (Yang et al., 2019; Yao, Wang, Gui, et al., 2017, Yao, Wang, Huang, et al., 2017).

3.2. Impact of Spatial Scale on SUHII Controls

Controls on the spatial variation of the SUHII tend to differ from those that control its temporal dynamics, yet they are also governed by scale (Figure 2). For the 5° × 5° and 10° × 10° scales, on average the

Figure 1. Relative importance of the three types of surface urban heat island intensity (SUHII) control on multiple temporal scales. The blue arrows in subplot a demonstrate the approach used to identify the coordinates of each point distribution. Sectors within the triangles with a large number of data points are highlighted in green, with the relative importance (rank) of SUHII controls represented by each sector illustrated in Figure S1. The blue and red lines adjacent to the axes represent the comparison of contribution from each of the three types of SUHII control in southern (i.e., tropical and subtropical) and northern (i.e., temperate) cities, with the central dots and line ranges denoting the means and standard deviations, respectively. The bar diagrams show the percentage of cities in which each of the three groups of factors makes the largest contribution to SUHII dynamics, wherein “wea.” (or “clm.”), “sur.”, and “urb.” represent the “weather or climate condition", “surface property” and “overall urban metric”, respectively. “TR”, “SS”, “MS”, “NS”, “PT”, “WT”, “AT”, “MT”, and “CT” denote tropical, south subtropical, mid subtropical, north subtropical, plateau temperate, warm temperate, arid temperate, mid temperate, and cold temperate climatic zones, respectively (see also Figure S2). Note that for the results over the day-to-day and daily scales, 12 city clusters were dropped, as there are less than 30 valid SUHII observations for regression due to the prevalence of clouds.

contributions from the overall urban metric (less than 20%) are lower than those from the other two SUHII control types (Figures 2a–2h). Over these two scales, the surface property is the main control for the daytime SUHII variations, whereas the nighttime SUHIIs are simultaneously controlled by climate condition and surface property. For the 15° × 15° scale, SUHII variations are regulated more by surface property during the day (Figures 2i and 2j). The average (±STD) contribution from surface property is 60% (±13%), while those from the other two types are both less than 30%. At night, the average (±STD) contribution from climatic condition increases: the value is 47% (±15%), comparable to that from surface property: 32% (±6%) (Figures 2k and 2l). Over the entire China, climatic condition makes the largest contribution (56% and 53% for daytime and nighttime; Figure 2), as background climate can impact vegetation activity and evaporative/convective effect over a large scale (Cao et al., 2016; D. Zhou et al., 2019). Although the individual contributions may vary, the results shown in Figure 2 demonstrate that city-by-city SUHII variations are controlled by combinations of the three types of factors, on all spatial scales. However, this is not the case for pixel-by-pixel SUHII variations within a single city, which can be explained primarily by surface property such as land cover type and landscape configuration (Weng et al., 2004; Yuan & Bauer, 2007); whereas the other two types of controls which vary mainly over a larger spatial scale (i.e., over the city-by-city or regional scale) show much smaller contributions. The relationships between pixel-based SUHII variations and surface property are also scale-dependent (Luan et al., 2020; J. Peng et al., 2020).

The differences between the dominant SUHII controls on different spatial scales show that it may be inappropriate to make a direct comparison among conclusions from previous studies that focused on the pixel-by-pixel (J. Li et al., 2021; Weng et al., 2004; Yuan & Bauer, 2007), regional (Du et al., 2016), sub-continental or continental (Shastri et al., 2017; Zhao et al., 2014; B. Zhou et al., 2013; D. Zhou et al., 2014), and global scales (Chakraborty & Lee, 2019; Manoli et al., 2019; S. Peng et al., 2012).

3.3. Impact of Sampling on SUHII Controls

The results shown in Figure 3 indicate that SUHII controls also depend on the criteria used for city selection. When city clusters are sampled based on a specific range of urban area, the spatial variations in SUHII are controlled mainly by climatic conditions (the mean contribution is 53% ± 23%), and then by surface property (36% ± 23%), rather than by overall urban metric (<15%). If sampled by climatic zone, SUHII variations are regulated more by surface property (the mean contribution is 53% ± 16%) during the day and by overall urban metric (40% ± 32%) at night, than by climatic conditions (<30% for both day and night).

Contributions from the overall urban metric on the SUHIIs, mainly via the increased anthropogenic heat release as well as by affecting the aerodynamic resistance and emissivity of urban surface (Manoli et al., 2019), was revealed to be larger over groups of larger city clusters (i.e., sample "UA10") than those of smaller city clusters (Figure 3). The contribution from the urban area also varies among city clusters with different ranges of urban area (Figure S8). This implies that SUHII controls may be sensitive to the urban size threshold used for city selection, although it is usual to select only large city clusters for analysis by setting a threshold based on urban area or population (X. Li et al., 2017; S. Peng et al., 2012; B. Zhou et al., 2013; D. Zhou et al., 2014).

Differences in SUHII controls with sampling criteria by climate zone are as significant as those by urban area. For instance, nighttime SUHII variations within cities in the SS (south subtropical) and MT (mid temperate) zones are more impacted by overall urban metrics than those within cities in the other climate zones (Figure 3). For the SS zone, the contributions from the overall urban metric reach 80%, 58%, and 74% in summer, winter, and all-year days, respectively; with the corresponding contributions of 70%, 73%, and 72% for the MT zone. The variations of SUHII controls by climate zone suggest that caution is needed in interpreting the major SUHII controls identified in regions with different climates, such as those in China (Cao et al., 2016; D. Zhou et al., 2014), India (Shastri et al., 2017), Europe (B. Zhou et al., 2013), and the USA (Zhao et al., 2014). They also imply that a comprehensive understanding of SUHII controls requires the inclusion of cities from a wide variety of climate zones (Chakraborty & Lee, 2019; Schwarz & Manceur, 2015).

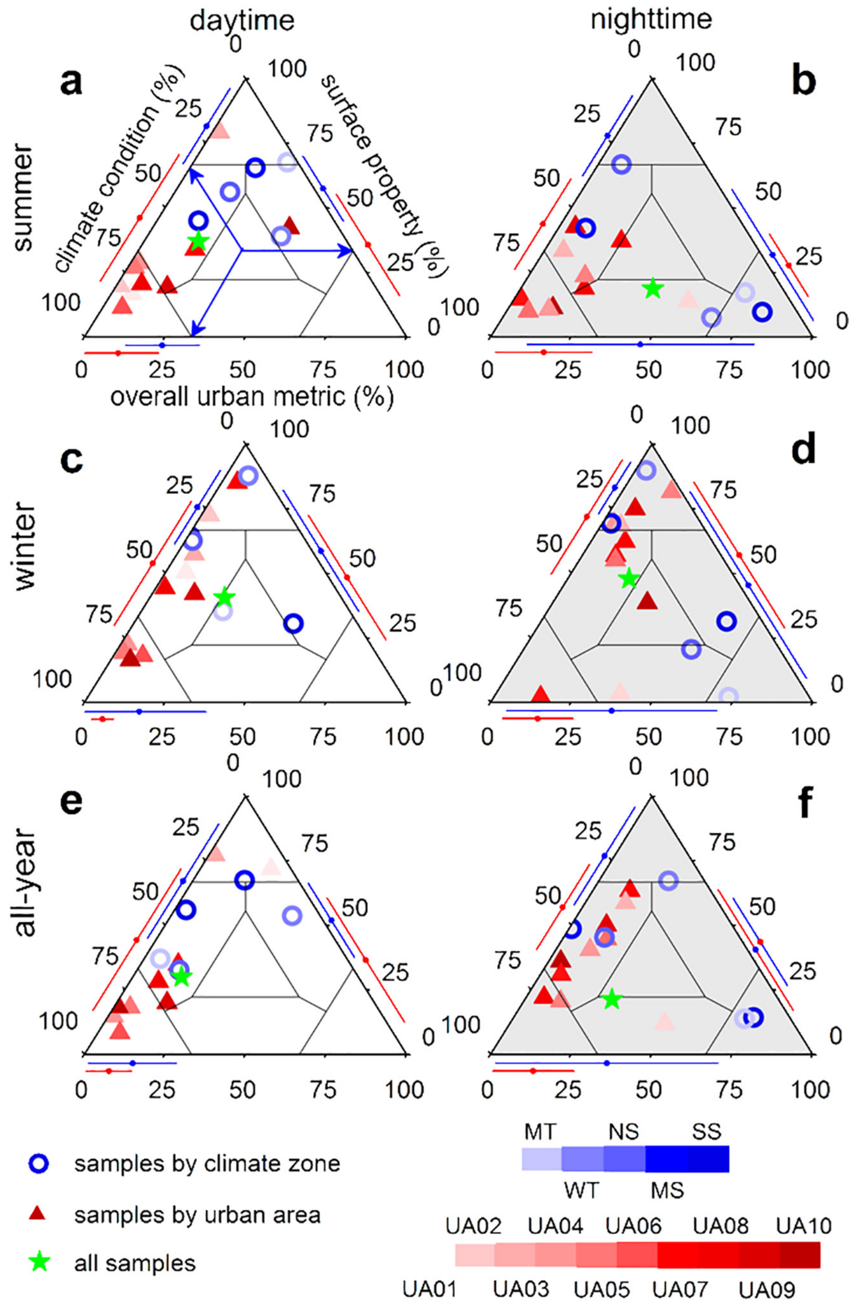

Figure 3. Dependence of surface urban heat island intensity (SUHII) controls on different sampling criteria. The blue and red lines adjacent to the axes represent the comparison of contribution from each of the three types of SUHII control using climate zone or urban area as the criteria for city selection, with the central dots and line ranges denoting means and standard deviations, respectively. "UA01" to "UA10" denote the 10 groups of city clusters with urban areas in the last 10 percentile to the top 10 percentile. The results in terms of sampling by climate zone are shown for only five climate zones where there are adequate city numbers for statistical attribution analysis.

3.4. Implications

Previous studies of SUHII controls have been handicapped by the insufficient attention paid to the scale of the investigation and the sampling criteria used for city clusters. The scale/sampling issue has been mentioned (D. Zhou et al., 2019), or partly addressed on the pixel-based scale (Luan et al., 2020; J. Peng et al., 2020). However, it remains unclear how and to what extent the neglect of investigation scale and sampling criteria would impact the interpretation of SUHII controls. Therefore, we conducted a comprehensive statistical analysis on the SUHII controls over 896 Chinese city clusters. The results show that with an increase in temporal scale (from day-to-day scale to daily/monthly and then to yearly scale), the contributions from climate (or weather) condition would decrease, whereas those from surface property and overall urban metric would increase. No consistent ranking of these three control types can be found on various spatial scales. Different sampling style of city cluster (by urban area or climate zone) would also lead to different ranks in SUHII controls. Our summarized SUHII controls over different scales (Table S6) and sampling criteria can provide reference for other studies on selecting variables to explain or simulate SUHII variations. More importantly, by ascribing the seemingly contradictory conclusions reached in the previous literature (Table S1) to the specific temporal/spatial scales and/or the sampling criteria employed, our results potentially help reconcile the long-standing debate on the relative importance of the main types of SUHII control.

Our findings alarm that inappropriate selection of scale and sampling criteria for city clusters will probably lead to an incomplete or even erroneous interpretation of SUHII controls. Conclusions regarding SUHII controls identified for a specific scale or sampling criterion should be made only in the context of that specific scale or sampling criterion and should not be generalized. Furthermore, while SUHII variations over certain scales/sampling criteria may be determined by only a few controls, a comprehensive investigation of SUHII controls should involve an adequate number of controls belonging to all the three main types of SUHII control.

Examination of the statistical relationship between SUHII and its controls is usually the first step toward understanding the underlying physical mechanisms and producing corresponding diagnostic equations (Cao et al., 2016; D. Li et al., 2019; Manoli et al., 2019; Zhao et al., 2014). Our results provide an improved understanding of the statistical attribution of SUHIIs. We acknowledge that statistical attribution is not a surrogate for physical attribution which can explain SUHII variations induced by radiative, evaporative, and convective processes (see Text S2). Nevertheless, our results provide a simple but efficient approach for rapidly identifying SUHII controls and for assessing their relative importance.

Conflict of Interest

The authors declare no conflicts of interest relevant to this study.

Data Availability Statement

The data sets used in this study are all publicly available: the city cluster boundary data set is publicly available at https://www.naturalearthdata.com/downloads/10m-cultural-vectors/10m-urban-area/; the population data set is publicly available at https://landscan.ornl.gov/landscan-datasets; the MODIS data sets are publicly available at https://e4ftl01.cr.usgs.gov/; while the reanalysis data are publicly available at https://apps.ecmwf.int/datasets/data/interim-full-daily/levtype=sfc/.

Acknowledgments
This research was jointly supported by the National Key R&D Program of China (2017YFA0603604), the Jiangsu Provincial Natural Science Foundation (BK20180009), and the National Natural Science Foundation of China (42171306). The authors are also grateful for the financial support provided by the National Youth Talent Support Program of China.

References

Cao, C., Lee, X., Liu, S., Schultz, N., Xiao, W., Zhang, M., & Zhao, L. (2016). Urban heat islands in China enhanced by haze pollution. *Nature Communications*, *7*(1), 1–7. https://doi.org/10.1038/ncomms12509

Chakraborty, T., & Lee, X. (2019). A simplified urban-extent algorithm to characterize surface urban heat islands on a global scale and examine vegetation control on their spatiotemporal variability. *International Journal of Applied Earth Observation and Geoinformation*, *74*, 269–280. https://doi.org/10.1016/j.jag.2018.09.015

Chen, X. L., Zhao, H. M., Li, P. X., & Yin, Z. Y. (2006). Remote sensing image-based analysis of the relationship between urban heat island and land use/cover changes. *Remote Sensing of Environment*, *104*(2), 133–146. https://doi.org/10.1016/j.rse.2005.11.016

Clinton, N., & Gong, P. (2013). MODIS detected surface urban heat islands and sinks: Global locations and controls. *Remote Sensing of Environment*, *134*, 294–304. https://doi.org/10.1016/j.rse.2013.03.008

Dee, D. P., Uppala, S. M., Simmons, A. J., Berrisford, P., Poli, P., Kobayashi, S., et al. (2011). The ERA-Interim reanalysis: Configuration and performance of the data assimilation system. *Quarterly Journal of the Royal Meteorological Society*, *137*(656), 553–597. https://doi.org/10.1002/qj.828

Dobson, J. E., Bright, E. A., Coleman, P. R., Durfee, R. C., & Worley, B. A. (2000). LandScan: A global population database for estimating populations at risk. *Photogrammetric Engineering & Remote Sensing*, *66*(7), 849–857.

Du, H., Wang, D., Wang, Y., Zhao, X., Qin, F., Jiang, H., & Cai, Y. (2016). Influences of land cover types, meteorological conditions, anthropogenic heat and urban area on surface urban heat island in the Yangtze River Delta urban agglomeration. *Science of the Total Environment*, *571*, 461–470. https://doi.org/10.1016/j.scitotenv.2016.07.012

Grimmond, S. U. (2007). Urbanization and global environmental change: Local effects of urban warming. *Geographical Journal*, *173*(1), 83–88. https://doi.org/10.1111/j.1475-4959.2007.232_3.x

Haashemi, S., Weng, Q., Darvishi, A., & Alavipanah, S. K. (2016). Seasonal variations of the surface urban heat island in a semi-arid city. *Remote Sensing*, *8*(4), 352. https://doi.org/10.3390/rs8040352

Heinl, M., Hammerle, A., Tappeiner, U., & Leitinger, G. (2015). Determinants of urban-rural land surface temperature differences—A landscape scale perspective. *Landscape and Urban Planning*, *134*, 33–42. https://doi.org/10.1016/j.landurbplan.2014.10.003

Hu, L. (2021). A global assessment of coastal marine heatwaves and their relation with coastal urban thermal changes. *Geophysical Research Letters*, *48*, e2021GL093260. https://doi.org/10.1029/2021gl093260

Huang, F., Zhan, W., Wang, Z. H., Voogt, J., Hu, L., Quan, J., et al. (2020). Satellite identification of atmospheric-surface-subsurface urban heat islands under clear sky. *Remote Sensing of Environment*, *250*, 112039. https://doi.org/10.1016/j.rse.2020.112039

Imhoff, M. L., Zhang, P., Wolfe, R. E., & Bounoua, L. (2010). Remote sensing of the urban heat island effect across biomes in the continental USA. *Remote Sensing of Environment*, *114*(3), 504–513. https://doi.org/10.1016/j.rse.2009.10.008

Lai, J., Zhan, W., Huang, F., Voogt, J., Bechtel, B., Allen, M., et al. (2018). Identification of typical diurnal patterns for clear-sky climatology of surface urban heat islands. *Remote Sensing of Environment*, *217*, 203–220. https://doi.org/10.1016/j.rse.2018.08.021

Lai, J., Zhan, W., Voogt, J., Quan, J., Huang, F., Zhou, J., et al. (2021). Meteorological controls on daily variations of nighttime surface urban heat islands. *Remote Sensing of Environment*, *253*, 112198. https://doi.org/10.1016/j.rse.2020.112198

Lazzarini, M., Marpu, P. R., & Ghedira, H. (2013). Temperature-land cover interactions: The inversion of urban heat island phenomenon in desert city areas. *Remote Sensing of Environment*, *130*, 136–152. https://doi.org/10.1016/j.rse.2012.11.007

Lazzarini, M., Molini, A., Marpu, P. R., Ouarda, T. B., & Ghedira, H. (2015). Urban climate modifications in hot desert cities: The role of land cover, local climate, and seasonality. *Geophysical Research Letters*, *42*(22), 9980–9989. https://doi.org/10.1002/2015gl066534

Li, D., Liao, W., Rigden, A. J., Liu, X., Wang, D., Malyshev, S., & Shevliakova, E. (2019). Urban heat island: Aerodynamics or imperviousness? *Science Advances*, *5*(4), eaau4299. https://doi.org/10.1126/sciadv.aau4299

Li, J., Zhan, W., Hong, F., Lai, J., Dong, P., Liu, Z., et al. (2021). Similarities and disparities in urban local heat islands responsive to regular-, stable-, and counter-urbanization: A case study of Guangzhou, China. *Building and Environment*, *199*, 107935. https://doi.org/10.1016/j.buildenv.2021.107935

Li, X., Zhou, Y., Asrar, G. R., Imhoff, M., & Li, X. (2017). The surface urban heat island response to urban expansion: A panel analysis for the conterminous United States. *Science of the Total Environment*, *605*, 426–435. https://doi.org/10.1016/j.scitotenv.2017.06.229

Liao, W., Liu, X., Wang, D., & Sheng, Y. (2017). The impact of energy consumption on the surface urban heat island in China's 32 major cities. *Remote Sensing*, *9*(3), 250. https://doi.org/10.3390/rs9030250

Logan, T. M., Zaitchik, B., Guikema, S., & Nisbet, A. (2020). Night and day: The influence and relative importance of urban characteristics on remotely sensed land surface temperature. *Remote Sensing of Environment*, *247*, 111861. https://doi.org/10.1016/j.rse.2020.111861

Luan, X. L., Yu, Z., Zhang, Y., Wei, S., Miao, X., Huang, Z. Y., et al. (2020). Remote sensing and social sensing data reveal scale-dependent and system-specific strengths of urban heat island determinants. *Remote Sensing*, *12*(3), 391. https://doi.org/10.3390/rs12030391

Luo, M., & Lau, N. C. (2018). Increasing heat stress in urban areas of eastern China: Acceleration by urbanization. *Geophysical Research Letters*, *45*(23), 13–60. https://doi.org/10.1029/2018gl080306

MacCallum, R. C., Widaman, K. F., Zhang, S., & Hong, S. (1999). Sample size in factor analysis. *Psychological Methods*, *4*(1), 84–99. https://doi.org/10.1037/1082-989x.4.1.84

Manoli, G., Fatichi, S., Schläpfer, M., Yu, K., Crowther, T. W., Meili, N., et al. (2019). Magnitude of urban heat islands largely explained by climate and population. *Nature*, *573*(7772), 55–60. https://doi.org/10.1038/s41586-019-1512-9

Oke, T. R., Mills, G., Christen, A., & Voogt, J. (2017). *Urban climate*. Cambridge University Press.

Peng, J., Jia, J., Liu, Y., Li, H., & Wu, J. (2018). Seasonal contrast of the dominant factors for spatial distribution of land surface temperature in urban areas. *Remote Sensing of Environment*, *215*, 255–267. https://doi.org/10.1016/j.rse.2018.06.010

Peng, J., Qiao, R., Liu, Y., Blaschke, T., Li, S., Wu, J., et al. (2020). A wavelet coherence approach to prioritizing influencing factors of land surface temperature and associated research scales. *Remote Sensing of Environment*, *246*, 111866. https://doi.org/10.1016/j.rse.2020.111866

Peng, S., Piao, S., Ciais, P., Friedlingstein, P., Ottle, C., Breon, F. M., et al. (2012). Surface urban heat island across 419 global big cities. *Environmental Science & Technology*, *46*(2), 696–703. https://doi.org/10.1021/es2030438

Scarano, M., & Sobrino, J. A. (2015). On the relationship between the sky view factor and the land surface temperature derived by Landsat-8 images in Bari, Italy. *International Journal of Remote Sensing*, *36*, 4820–4835. https://doi.org/10.1080/01431161.2015.1070325

Schwarz, N., & Manceur, A. M. (2015). Analyzing the influence of urban forms on surface urban heat islands in Europe. *Journal of Urban Planning and Development*, *141*, A4014003. https://doi.org/10.1061/(asce)up.1943-5444.0000263

Shaposhnikova, M. (2018). *The influence of wind speed on nighttime surface temperatures and the surface urban heat island of Phoenix AZ*. MSc. Thesis, Western University.

Shastri, H., Barik, B., Ghosh, S., Venkataraman, C., & Sadavarte, P. (2017). Flip flop of day-night and summer-winter surface urban heat island intensity in India. *Scientific Reports*, *7*(1), 1–8. https://doi.org/10.1038/srep40178

Voogt, J. A., & Oke, T. R. (2003). Thermal remote sensing of urban climates. *Remote Sensing of Environment*, *86*, 370–384. https://doi.org/10.1016/s0034-4257(03)00079-8

Wan, Z. (2008). New refinements and validation of the MODIS land-surface temperature/emissivity products. *Remote Sensing of Environment*, *112*, 59–74. https://doi.org/10.1016/j.rse.2006.06.026

Wang, J., Huang, B., Fu, D., & Atkinson, P. M. (2015). Spatiotemporal variation in surface urban heat island intensity and associated determinants across major Chinese cities. *Remote Sensing*, *7*(4), 3670–3689. https://doi.org/10.3390/rs70403670

Ward, K., Lauf, S., Kleinschmit, B., & Endlicher, W. (2016). Heat waves and urban heat islands in Europe: A review of relevant drivers. *Science of the Total Environment*, *569*, 527–539. https://doi.org/10.1016/j.scitotenv.2016.06.119

Weng, Q. (2009). Thermal infrared remote sensing for urban climate and environmental studies: Methods, applications, and trends. *ISPRS Journal of Photogrammetry and Remote Sensing*, *64*, 335–344. https://doi.org/10.1016/j.isprsjprs.2009.03.007

Weng, Q., Lu, D., & Schubring, J. (2004). Estimation of land surface temperature-vegetation abundance relationship for urban heat island studies. *Remote Sensing of Environment*, *89*, 467–483. https://doi.org/10.1016/j.rse.2003.11.005

Yang, Q., Huang, X., & Tang, Q. (2019). The footprint of urban heat island effect in 302 Chinese cities: Temporal trends and associated factors. *Science of the Total Environment*, *655*, 652–662. https://doi.org/10.1016/j.scitotenv.2018.11.171

Yang, X., Ruby Leung, L., Zhao, N., Zhao, C., Qian, Y., Hu, K., et al. (2017). Contribution of urbanization to the increase of extreme heat events in an urban agglomeration in East China. *Geophysical Research Letters*, *44*(13), 6940–6950. https://doi.org/10.1002/2017gl074084

Yao, R., Wang, L., Gui, X., Zheng, Y., Zhang, H., & Huang, X. (2017). Urbanization effects on vegetation and surface urban heat islands in China's Yangtze River Basin. *Remote Sensing*, *9*(6), 540. https://doi.org/10.3390/rs9060540

Yao, R., Wang, L., Huang, X., Gong, W., & Xia, X. (2019). Greening in rural areas increases the surface urban heat island intensity. *Geophysical Research Letters*, *46*(4), 2204–2212. https://doi.org/10.1029/2018gl081816

Yao, R., Wang, L., Huang, X., Niu, Z., Liu, F., & Wang, Q. (2017). Temporal trends of surface urban heat islands and associated determinants in major Chinese cities. *Science of the Total Environment*, *609*, 742–754. https://doi.org/10.1016/j.scitotenv.2017.07.217

Yow, D. M. (2007). Urban heat islands: Observations, impacts, and adaptation. *Geography Compass*, *1*, 1227–1251. https://doi.org/10.1111/j.1749-8198.2007.00063.x

Yuan, F., & Bauer, M. E. (2007). Comparison of impervious surface area and normalized difference vegetation index as indicators of surface urban heat island effects in Landsat imagery. *Remote Sensing of Environment*, *106*, 375–386. https://doi.org/10.1016/j.rse.2006.09.003

Zhao, L., Lee, X., Smith, R. B., & Oleson, K. (2014). Strong contributions of local background climate to urban heat islands. *Nature*, *511*(7508), 216–219. https://doi.org/10.1038/nature13462

Zheng, J., Yin, Y., & Li, B. (2010). A new scheme for climate regionalization in China. *Acta Geographica Sinica*, *65*(1), 3–13.

Zhou, B., Rybski, D., & Kropp, J. P. (2013). On the statistics of urban heat island intensity. *Geophysical Research Letters*, *40*, 5486–5491. https://doi.org/10.1002/2013gl057320

Zhou, B., Rybski, D., & Kropp, J. P. (2017). The role of city size and urban form in the surface urban heat island. *Scientific Reports*, *7*(1), 1–9. https://doi.org/10.1038/s41598-017-04242-2

Zhou, D., Xiao, J., Bonafoni, S., Berger, C., Deilami, K., Zhou, Y., et al. (2019). Satellite remote sensing of surface urban heat islands: Progress, challenges, and perspectives. *Remote Sensing*, *11*(1), 48.

Zhou, D., Zhao, S., Liu, S., Zhang, L., & Zhu, C. (2014). Surface urban heat island in China's 32 major cities: Spatial patterns and drivers. *Remote Sensing of Environment*, *152*, 51–61. https://doi.org/10.1016/j.rse.2014.05.017

Zhou, J., Chen, Y., Wang, J., & Zhan, W. (2011). Maximum nighttime urban heat island (UHI) intensity simulation by integrating remotely sensed data and meteorological observations. *IEEE Journal of Selected Topics in Applied Earth Observations and Remote Sensing*, *4*(1), 138–146. https://doi.org/10.1109/jstars.2010.2070871

Zhou, L., Dickinson, R. E., Tian, Y., Fang, J., Li, Q., Kaufmann, R. K., et al. (2004). Evidence for a significant urbanization effect on climate in China. *Proceedings of the National Academy of Sciences*, *101*(26), 9540–9544. https://doi.org/10.1073/pnas.0400357101

Zhou, W., Huang, G., & Cadenasso, M. L. (2011). Does spatial configuration matter? Understanding the effects of land cover pattern on land surface temperature in urban landscapes. *Landscape and Urban Planning*, *102*, 54–63. https://doi.org/10.1016/j.landurbplan.2011.03.009

References From the Supporting Information

Breiman, L., Friedman, J., Stone, C. J., & Olshen, R. A. (1984). *Classification and regression trees*. CRC press.

Deilami, K., Kamruzzaman, M., & Liu, Y. (2018). Urban heat island effect: A systematic review of spatio-temporal factors, data, methods, and mitigation measures. *International Journal of Applied Earth Observation and Geoinformation*, *67*, 30–42. https://doi.org/10.1016/j.jag.2017.12.009

Huang, Y., Yuan, M., & Lu, Y. (2017). Spatially varying relationships between surface urban heat islands and driving factors across cities in China. *Environment and Planning B: Urban Analytics and City Science*, *46*, 377–394. https://doi.org/10.1177/2399808317716935

James, G., Witten, D., Hastie, T., & Tibshirani, R. (2013). *An introduction to statistical learning*. Springer.

Quan, J., Chen, Y., Zhan, W., Wang, J., Voogt, J., & Wang, M. (2014). Multi-temporal trajectory of the urban heat island centroid in Beijing, China-based on a Gaussian volume model. *Remote Sensing of Environment*, *149*, 33–46. https://doi.org/10.1016/j.rse.2014.03.037

Zhou, D., Zhang, L., Li, D., Huang, D., & Zhu, C. (2016). Climate-vegetation control on the diurnal and seasonal variations of surface urban heat islands in China. *Environmental Research Letters*, *11*(7), 074009. https://doi.org/10.1088/1748-9326/11/7/074009